Journal Pre-proofs

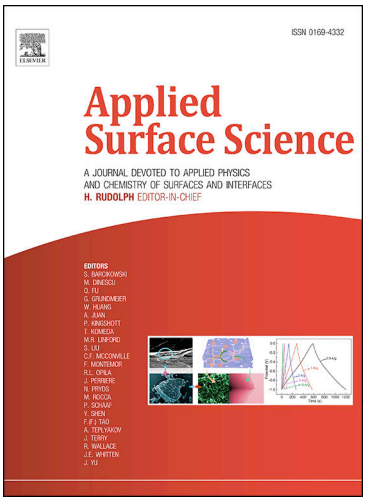

Full Length Article

Thermal evolution and migration behavior of ion-implanted nitrogen in ZnO:In-N films

Hong Zhang, Wanjun Li, Guoping Qin, Haibo Ruan, Dong Wang, Jiang Wang, Zheng Huang, Fang Wu, Chunyang Kong, Liang Fang

PII: S0169-4332(19)33609-8
DOI: https://doi.org/10.1016/j.apsusc.2019.144793
Reference: APSUSC 144793

To appear in: *Applied Surface Science*

Received Date: 5 August 2019
Revised Date: 16 October 2019
Accepted Date: 18 November 2019

Please cite this article as: H. Zhang, W. Li, G. Qin, H. Ruan, D. Wang, J. Wang, Z. Huang, F. Wu, C. Kong, L. Fang, Thermal evolution and migration behavior of ion-implanted nitrogen in ZnO:In-N films, *Applied Surface Science* (2019), doi: https://doi.org/10.1016/j.apsusc.2019.144793

Thermal evolution and migration behavior of ion-implanted nitrogen in ZnO:In-N films

Hong Zhang[1, 2, *], Wanjun Li[2, *†], Guoping Qin[2], Haibo Ruan[3], Dong Wang[2], Jiang Wang[2], Zheng Huang[1], Fang Wu[1], Chunyang Kong[2], Liang Fang[1, 4†]

[1] *State Key Laboratory of Power Transmission Equipment & System Safety and New Technology, Chongqing Key Laboratory of Soft Condensed Matter Physics and Smart Materials, College of Physics, Chongqing University, Chongqing 400044, P.R. China*

[2] *Chongqing Key Laboratory of Photo-Electric Functional Materials, College of Physics and Electronic Engineering, Chongqing Normal University, Chongqing 401331, P.R. China*

[3] *Research Center for Materials Interdisciplinary Sciences, Chongqing University of Arts and Sciences, Chongqing 402160, P.R. China*

[4] *State Key Laboratory of Luminescence and Applications, Changchun Institute of Optics, Fine Mechanics and Physics, Chinese Academy of Sciences, No.3888 Dong Nanhu Road, Changchun, Jilin, 130033, P.R. China*

* Hong Zhang and Wanjun Li contributed equally to this work;

† Prof. Wanjun Li, E-mail: liwj@cqnu.edu.cn, Tel.: +86 23 65362779;

† Prof. Liang Fang, E-mail: lfang@cqu.edu.cn, Tel.: +86 23 65678369.

Abstract

Thermal evolution and migration behavior of nitrogen (N) dopants in indium (In) doped ZnO films implanted with high-dose N ions (ZnO:In-N) were investigated by means of experiment and first-principles calculations. The results demonstrate that N-dopants have poor thermal stability, which has a significant impact on N local chemical states. In particular, two different temperature region s can clearly be distinguished in the annealing process. At low-temperature region, the interaction of substitutional nitrogen (N_O) acceptor and interstitial nitrogen (N_i) starts to occur, which leads to a decrease in N_O acceptor and the formation of additional molecular nitrogen at oxygen site [$(N_2)_O$]. In contrast, at high-temperature region, annealing favors energetically the generation of abundant oxygen vacancies near the surface and simultaneously induces the serious out-diffusion of N-dopants. Combined with the calculated migration barriers, oxygen vacancies are deemed to assist the out-diffusion of N-dopants via a vacancy mechanism. This work provides insights into the formation and evolution of different N-related defects and their interaction with intrinsic defects.

Keywords: ZnO thin films, nitrogen dopants, vacancy mechanism, thermal stability, migration

1. Introduction

ZnO is a potentially important semiconductor material for short-wavelength optoelectronic devices due to its large exciton binding energy of 60 meV and wide direct band gap of 3.37 eV at room temperature [1]. However, the notoriously doping asymmetry problem causes the stable, reproducible p-type doping of ZnO to remain a major challenge [2, 3]. Among the group V elements, nitrogen (N) is considered to be the most promising candidate for acceptor doping because of its similar atomic size and electronegativity to oxygen (O) [4]. Experimentally, researchers have made great efforts to realize p-type conductivity and even confirmed homogeneous pn-junction based on N-doped ZnO [5, 6]. Nevertheless, the shallow acceptor nature of N in ZnO is still controversial [7, 8]. Recently, several co-doping strategies (including Li/Na-N co-doping [9, 10], Al/Ga/In-N co-doping [11-13], Be/Mg/Te-N co-doping [14-17], etc.) have been proposed and experimentally demonstrated, not only improving the solid solubility but also reducing the acceptor ionization energy [18].

It is well known that the thermal stability of dopants directly determines the reliability of the device operation. In the case of N doped ZnO, the weak chemical bond between the N and Zn can easily lead to thermal instability of N-dopants, causing p-type conductivity performance to decay or even convert to n-type over time [19, 20]. Similar results have recently been declared in Na-doped ZnO [21]. The substitutional Na acceptors gradually transform into donors by high-temperature annealing or when the crystals are aged [21]. Actually, Fons et al. have directly observed the metastability of the N acceptors and the formation of molecular nitrogen upon annealing as early as 2006 [22]. Subsequently, Liu et al. detected the effect of annealing temperature on the N local chemical states through in-situ temperature-dependent XPS measurement, concluding that N dopants have poor thermal stabilities [23]. Recently, Chen et al. reported that the simultaneous incorporation of a small amount of Be element can improve

the thermal stability and solid solubility of N dopants in N-doped ZnO, and the corresponding p–i–n junction LED device can operate at temperatures as high as 400 K [14, 15]. In addition, the obvious N-dopants loss phenomenon was also observed at elevated temperatures [24]. Up to now, the poor thermal stability of N in ZnO is far from being comprehensively understood, and even little attention has been paid to the annealing effect on the migration of N-dopants in ZnO. Therefore, understanding thermal evolution of dopants, especially N, is of primary importance for improving p-type doping efficiency, determining their annealing temperatures and realizing high-temperature operation of ZnO-based optoelectronic devices.

In this work, we focus on the effect of post-implantation annealing temperature on thermal evolution and migration behavior of N-dopants in indium doped ZnO films implanted with high-dose nitrogen ions. The comprehensive investigation reveals that N-dopants have poor thermal stability and the evolution of nitrogen local environment strongly depends on the post-implantation annealing temperature. In addition, employing the climbing image nudged elastic band method (CI-NEB), we calculated the migration barriers of N-related defects and identified the diffusion mechanisms of N-dopants by oxygen vacancies.

2. Material and methods

Indium-nitrogen codoped ZnO thin films were prepared by two-step method. Firstly, indium doped ZnO (ZnO:In) thin films were deposited on quartz substrates by radio frequency magnetron sputtering at room temperature. A disk of commercial ZnO ceramic sputtering target with indium content of 1 at.% was supplied by China New Metal Materials Technology Co., Ltd. The detailed process and parameters of ZnO:In thin films can be found elsewhere [25]. The sputtering time is controlled at 40 minutes and the corresponding thickness of ZnO:In thin film is about 500 nm. Then, heavily doped ZnO:In-N thin films were achieved by implanting N ion beam into ZnO:In thin films with energy of 70 keV and a high dose of 1.0×10^{17} ions/cm^2 at room temperature. Following N ion implantation, the ZnO:In-N film was cut into five pieces. Four of them underwent isochronal post-annealing in a vacuum environment for 30 min at various annealing temperatures (T_A=400 °C, 600°C, 700 °C and 800 °C, respectively), and the remaining piece as a reference was not subjected to any heat treatment.

The crystalline structure of the implanted samples before and after annealing was characterized by X-ray diffraction (XRD) measurements with a Cu $K_{\alpha 1}$ radiation source (λ =1.540598 Å). X-ray photoelectron spectroscopy (XPS) measurements were carried out with ESCALAB 250 using a monochromatic Al K_α source (15 kV, 150W) and all binding energies have been calibrated by the C 1*s* peak at 284.6 eV. The depth profile of nitrogen dopants in ZnO:In-N films was investigated by secondary ion mass spectroscopy (SIMS) with 1 keV Cs^+-ions as the primary beam. All measurements were conducted at room temperature.

The calculations within density functional theory were carried out with the Vienna Ab initio Simulation Package (VASP) [26]. The generalized gradient approximation (GGA) within Perdew−Burke−Ernzerhof (PBE) formalism is employed for the exchange and correlation potential [27].

The projector augmented wave (PAW) method is used to take into account the electron–ion interaction [28]. A plane-wave basis set with an energy cutoff of 400 eV is used in the calculations. We employed a 4×4×2 supercell geometry containing 128 host atoms for the wurtzite structure and a set of k points generated by the 2×2×2 Monkhorst–Pack mesh for Brillouin-zone integration. In geometry optimization, the energy convergence with the energy difference is below 10^{-5} eV between two consecutive self-consistent steps while the positions of all the atoms in the supercell were fully relaxed until the force was less than 0.02 eV/Å. The climbing image nudged elastic band method (CI-NEB) [29] was used to find the minimum energy pathway and diffusion barriers for Nitrogen diffusion in ZnO. Initial and final configurations were first fully optimized before the CI-NEB calculation. After that, five images were linearly interpolated between them. The images were relaxed until the maximum residual force was less than 0.05 eV/Å.

3. Results

Fig. 1 illustrates the XRD patterns of as-implanted and post-annealed ZnO:In-N films. All of them display a strong preferential diffraction peak at ~34.56° corresponding to the (002) plane of typical ZnO wurtzite structure (**JCPDS#36-1451**), and no other impurity phases (such as Zn_3N_2, In_2O_3 or InN) are detected. For the films annealed at low temperatures (not exceeding 600 °C), the intensity of (002) diffraction peaks is higher than that of as-implanted film, implying that the crystallinity of ZnO:In-N films can be effectively improved by appropriate thermal treatment. Upon further increasing annealing temperature (T_A>600 °C), the intensity of (002) diffraction peak gradually becomes less intense. It is highly likely that high-temperature annealing leads to the near surface degradation of the ZnO:In-N film, as this was already reported by other studies [30, 31]. Moreover, the (002) diffraction peaks of post-

annealed ZnO:In-N films show an obvious shift to a large angle with respect to that of as-implanted sample. The shift of (002) diffraction peaks generally ascribes to the changed biaxial stress in the film after post-annealing due to the local non-uniformity in the film, which involves local defects or impurities [32].

Furthermore, the XPS measurements are utilized to examine the chemical state of elements in ZnO:In-N films. **Fig. S1** (Supporting Information) shows the high resolution Zn 2*p*, In 3*d*, O 1*s* and N 1*s* XPS spectra of as-implanted and post-annealed ZnO:In-N samples, which confirm that In and N have been successfully incorporated into ZnO films. Notably, the chemical state of N and O shows dramatic changes with increasing annealing temperature, implying that annealing temperature has a significant effect on the evolution of N and O local chemical states. Specifically, the O 1*s* XPS spectra have been consistently fitted by three Gaussian components of variable intensities, as shown in **Figs. 2(a-e)**. The typical binding energy values are located at 530.2±0.1 eV (denoted by O_I), 531.7±0.1 eV (denoted by O_{II}) and 533±0.1 eV (denoted by O_{III}), respectively. The low binding energy component (O_I) is associated with O^{2-} ions in the ZnO crystal lattice surrounded by Zn^{2+} [33]. The high binding energy component (O_{III}) is attributed to the presence of loosely bound oxygen on the surface of ZnO [34, 35]. The medium binding energy component (O_{II}) usually is attributed to the presence of the O atoms in the oxygen deficiency region, which can be correlated with oxygen vacancies in the ZnO crystal lattice [33, 34, 36]. Therefore, changes in the intensity of the O_{II} component can be used to describe semi-quantitatively the variations in the concentration of oxygen vacancies near surface of the film. **Fig. 2f** shows the variation of the integral areas ratio (O_{II}/O_I) with annealing temperature (T_A). The integral area ratio of O_{II}/O_I for ZnO:In-N films annealed at 400 °C is slightly lower than that of as-implanted ZnO:In-N films. It suggests that the oxygen vacancies of ZnO:In-N films were reduced when annealed at 400 °C, which can be

considered as the improved crystallinity after annealing. Furthermore, the integral area ratio (O_{II}/O_I) increases monotonically as the annealing temperature increases from 400 to 800 °C, suggesting the formation of new oxygen vacancies near the surface of ZnO:In-N films (especially at T_A = 800 °C). This is consistent with previous studies that heat treatment gives rise to the loss of near-surface oxygen atoms [37, 38], thereby leaving abundant oxygen vacancies [39-41].

To identify the evolution of chemical states and the thermal stability of N-dopants in the ZnO:In-N films, we compares the N 1*s* XPS spectra of as-implanted and post-annealed ZnO:In-N films. The N 1*s* XPS spectra have been fitted with different Gaussian-Lorentzian peak shapes, as shown in **Figs. 3(a-e)**. For the as-implanted ZnO:In-N film, only two deconvoluted N 1*s* XPS peaks, centered near the binding energy of ~ 396.0 eV (N_I) and ~ 403.5 eV (N_{III}), respectively, can be clearly identified (see **Fig. 3a**). The N_I peak usually appears in heavily N-doped ZnO [42, 43] and its position is very close to the binding energy of N-Zn bond in Zn_3N_2 [44]. Considering that high dose N-ion implantation is implemented in this work, the observed N_I peak should be ascribed to nitrogen on oxygen sites (N_O) located in N-rich local environments [23]. It indicates that part of N-dopants have been successfully incorporated into the O sites of ZnO via ion implantation. Moreover, the peak located at ~ 403.5 eV can be also observed in as-implanted ZnO:In-N sample, which has been known as molecular nitrogen on oxygen sites [$(N_2)_O$] [42]. Thus, both N_O acceptors and $(N_2)_O$ donors can be generated simultaneously during the high dose N ion implantation process. Interestingly, a new peak located ~ 398.8 eV (N_{II}) appeared when the annealing temperature reaches up to 600 °C, as shown in **Fig. 3c**. The binding energy value of N_{II} peak is close to that reported by Li et al. [23]. Unlike the assignment of N_I peak (396 eV), the N_{II} peak has been assigned to the N_O acceptor in O-rich local environments [23], in other words, meaning that only a few oxygen lattice sites are occupied by N atoms. Therefore, the N_{II} peak at 398.8

eV could be tentatively considered as N_O acceptor located in N-deficient local environment, the emergence of which can be further supported by the subsequent SIMS measurements.

The variation of the integral area of corresponding N 1*s* XPS peaks with annealing temperature is illustrated in **Fig. 3f**. Clearly, two different temperature region for the evolution of N chemical states can be clearly distinguished in the annealing process. For the films annealed at low temperature region (not exceeding 600 °C), as the annealing temperature increases, the integral area of N_I peak at 396.0 eV decreases slowly while the integral area of N_{III} peak at 403.5 eV gradually becomes larger, implying that additional $(N_2)_O$ donors are generated while N_O acceptors in N-rich local environment decrease. However, the local chemical state of N-dopants changes dramatically at the high temperature low temperature region (above 600 °C). The N_{III} peak disappears when the annealing temperature is increased to 700 °C. Additionally, the integral area of N_I peak decreases sharply with increasing temperatures. Conversely, the N_{II} peak becomes progressively stronger and eventually dominates the N 1*s* XPS spectrum at 800 °C, as shown in **Fig. 3e**. That is, the vacuum high-temperature annealing could promote the rapid transition from N-rich local environment to N-deficient local environment.

As is well-known, the detection depth of XPS is only several nanometers. Thus, SIMS was employed as a supplementary method to investigate the depth profile of N-dopants in samples before and after annealing. The curves in **Fig. 4** show the relative nitrogen concentration versus depth profiles in ZnO:In-N films with annealing temperature. In this work, the $^{14}N^{16}O^-$ signal was examined to monitor the distributions of N-dopants in the sample. It can be seen that the distribution of N-dopants does not show significant changes in the range of 0-250 nm when the annealing temperature does not exceed 600 °C. The distribution of N-dopants becomes more uniform for sample annealed at 600 °C. However, the further increase of annealing temperature (above 600 °C) leads to an overall decline of $^{14}N^{16}O^-$ signal

in the range of 0-250 nm. The higher the annealing temperature is, the more serious the $^{14}N^{16}O^-$ signal loss will be. Especially, the $^{14}N^{16}O^-$ signal drops sharply in the 0-100 nm region at 800 °C. It is noteworthy that we do not observe substantial N diffusion towards the inside of ZnO:In-N films at the depths of 250-350 nm when annealing at 400~800 °C, but the movement of the total N profile towards the film surface. Thus, it can be deduced that the continuous out-diffusion of N dopants from the substrate to the surface leads to the decline of $^{14}N^{16}O^-$ signal, which well supported the emergence of N-deficient local environment near the surface at elevated temperature region. Based on the above discussion, our results indicate that N-dopants in ZnO:In-N film have poor thermal stability and the evolution of nitrogen local environment strongly depends on the annealing temperature.

4. Discussion

The above experimental results have confirmed that N-dopants do not have good thermal stability. According to **Fig. 3f** and **Fig. 4**, the evolutionary behavior of N-dopants can be divided into two different temperature region: a low temperature region ($T_A \leq 600$ °C) and a high temperature region ($T_A > 600$°C). The following theoretical calculations will be implemented to explain the possible evolution mechanism of N-dopants at different annealing region.

Low temperature region: SIMS measurement reveals that annealing has little effect on the distribution of nitrogen concentration in samples at annealing temperature below 600 °C, as shown in **Fig. 4**. However, the evolution of N local chemical state depends strongly on annealing temperatures. It can be seen from **Fig. 3f** that low temperature annealing increases the content of $(N_2)_O$ donors, but conversely decreases the content of N_O acceptors, which seems to imply that annealing facilitates the transformation from N_O acceptors to $(N_2)_O$ donors. Here, two possibilities may be proposed to explain

the thermal evolution of N local chemical state, which will be discussed in the following discussion section. The first is the interaction between two adjacent N_O acceptors to form the $(N_2)_O$ donor. The second is based on the migration of nitrogen interstitial (N_i) and subsequent interaction with the neighboring N_O acceptor to form the $(N_2)_O$ donor.

First of all, we considered that the formation of $(N_2)_O$ donor by two adjacent N_O acceptors. **Figs. 5(a-b)** present the interaction between two adjacent N_O acceptors via the first out of (0001) plane and the first in (0001) plane, respectively. The corresponding diffusion energy barriers are only 1.51 eV and 1.36 eV, respectively. However, the formed $(N_2)_O$ configurations are highly metastable and will easily dissociate back to two adjacent N_O acceptors due to the small activation barriers of 0.88 eV and 0.8 eV. Therefore, the formation of **$(N_2)_O$** donor by two adjacent **N_O** acceptors is energetically unfavorable.

It is worth noting that N-doping by ion implantation will inevitably lead to a large amount of N-dopants occupying the interstitial sites. Previous literature reports that nitrogen interstitial has two configurations: nitrogen interstitial at octahedral site (**oct-N_i**) and split nitrogen interstitial (**split-N_i**), respectively. The former is in the metastable configuration and has a low migration barrier, while the latter is relatively stable and can bond with the lattice oxygen to form $(NO)_O$ configuration [45]. Therefore, we believe that the latter should be abundantly present in the as-implanted ZnO:In-N samples. The possible formation process of **$(N_2)_O$** donor by interactions between **N_O** acceptor and split-N_i is shown in **Fig. 5c**. It can be seen that split-N_i tends to bond with N_O acceptor to form **$(N_2)_O$** donor when split-N_i is present near No acceptor because the barrier to overcome only needs 1.85 eV. On the contrary, the dissociation of **$(N_2)_O$** into No and split-N_i needs to overcome a considerable barrier of 4.43 eV (**see Fig. 5c**). Thus, the formation of $(N_2)_O$ donors by the combination of N_O acceptor and split-N_i is energetically favorable. Experimentally, the above XPS measurements indicate that the increase of **$(N_2)_O$** donors has

already appeared at 400 °C, and the corresponding activation barrier is about 1.75 eV [46]. Our calculated value of 1.85 eV is in good agreement with the experimental result. Therefore, we believe that the migration behavior of split-N_i is likely to lead to the transformation from N_O acceptors to **$(N_2)_O$** donors at low temperature region.

High temperature region: As discussed in SIMS, high temperature annealing promotes the out-diffusion of abundant N-dopants, which leads to the transition from N-rich local environment to N-deficient local environment. Our previous work has shown that the diffusion energy barrier of split-N_i atom via an interstitial mechanism is up to 2.25 eV and the corresponding annealing temperature needs about 600 °C [47]. However, the above calculation results further reveal that split-N_i is more likely to be captured by No defects to form $(N_2)_O$ donors during the diffusion process due to the low migration barrier of 1.85 eV (see **Fig. 5c**). Thus, it can be considered that only a small amount of split-N_i may escape from the film. On the other hand, the isolated N_O acceptor defects are almost impossible to dissociate from the lattice sites to form interstitial N atoms, because this process needs to overcome a very large barrier of 5.51 eV [47]. Therefore, there should be other diffusion pathway for the out-diffusion of N-dopants. Actually, the present work has shown that a large number of newly generated V_O defects appear when N-dopants diffuse outward at high temperature region, as shown in **Fig. 2f**. Whether there is a close relationship between the oxygen vacancies and the out-diffusion of N-dopants deserves further investigation.

For this purpose, we first investigated the diffusion behavior of isolated V_O defects in ZnO. As can be seen from **Fig. 6a**, there are two kinds of nonequivalent pathways for the migration of isolated V_O defects by exchanging with its neighboring O atom: the diffusion path "B→A" is the first out of (0001) plane and the diffusion path "B→C" is the first in (0001) plane. The calculated energy barriers are

2.44 eV and 2.79 eV for the isolated V_O via the first in (0001) plane and the first out of (0001) plane, respectively, as shown in **Fig. 6b**. The larger diffusion barriers indicate that the oxygen vacancies become mobile at a relatively high temperature [46]. Surprisingly, when N_O is present near the V_O, the calculated activation energy barriers for N_O exchanging with V_O are found to be only 0.97 eV and 1.59 eV via different diffusion paths, as shown in **Fig. 6c**. Obviously, in the presence of N_O defects, V_O is quite easy to exchange position with neighboring nitrogen, which allows the diffusion of internal N_O defects via the neighboring vacancy. Experimentally, the O 1*s* XPS spectra (see **Fig. 2f**) confirmed that vacuum high-temperature annealing brings about a large amount of oxygen vacancies near surface area that are expected to diffuse into film at a relatively high temperature, which provides a favorable condition for the out-diffusion of N_O defects.

Furthermore, taking the effect of the nearest neighboring In_{Zn} into account, we further investigated the activation energy barriers for N_O exchanging with V_O in In-N codoped ZnO films. **Fig. S2(a-b)** show the different diffusion path of N-dopants escaping from Indium under different configurations. ①-④ sites represent the possible location of the V_O defects. For convenience, the corresponding diffusion path are labeled 1, 2, 3 and 4, respectively. Obviously, the calculated diffusion energy barrier is between 1.71 eV and 1.99 eV [see **Fig. S2(c)**], which is slightly higher than that of the absence of Indium. The corresponding thermal activation temperature is in the range of 656 to 764 K. The calculation results show that Indium can stabilize the nitrogen acceptors in ZnO to a certain extent, if the In-N bond is formed, similar to the results reported by Wang et al. [48]. Even so, high temperature annealing (T_A > 600 °C) will still cause the dissociation of In-N bond. Based on the above discussion, we believe that the generated oxygen vacancies continuously exchange with internal N_O defects in the film, and then the N_O defects will continuously diffuse out via oxygen vacancy-assisted diffusion

mechanism at high temperature annealing region.

Similarly, whether or not $(N_2)_O$ donors can also diffuse directly through a vacancy-assisted process, thus causing the disappearance of $(N_2)_O$ donors at high temperature. For this purpose, we investigated the diffusion behavior of $(N_2)_O$ via V_O-assisted diffusion mechanism, as shown in **Fig. 7**. However, such a high migration barrier of 2.98 eV does not support this diffusion behavior at the current annealing temperature. Additionally, we note that once V_O is located near the $(N_2)_O$ configuration, this configuration will easily dissociate back to two adjacent N_O acceptors [see the reverse process in **Fig. 5(a-b)**]. Thus, if the $(N_2)_O$ configuration encounters an oxygen vacancy, $(N_2)_O$ will first dissociate into two adjacent N_O acceptors. Then, these newly formed N_O acceptors will continue to spread out through the vacancy-assisted diffusion mechanism. Therefore, the vacancy-assisted diffusion mechanism dominates the out-migration of N-dopants and facilitates the appearance of N-deficient local environment at elevated temperature region.

5. Conclusion

In summary, we have investigated the thermal evolution and migration behavior of N-dopants in heavily doped ZnO:In-N films at different annealing temperatures combining experimental research and theoretical calculations. It is found that nitrogen dopants do not have good thermal stability. At a low temperature region ($T_A \leq 600$ °C), the interaction between N_O acceptor and split-N_i not only forms compensatory $(N_2)_O$ donor defects but also reduces N_O acceptors. However, at a high temperature region ($T_A > 600$ °C), lots of V_O concentration near the surface began to appear. As a result, nitrogen dopants will experience serious out-diffusion via oxygen vacancy assisted diffusion mechanism, leading to the destruction of $(N_2)_O$ donors and the appearance of N-deficient local environment. Therefore, improving

thermal stability of N dopants should be a non-negligible aspect for achieving stable and high quality p-type ZnO semiconductors.

Acknowledgments

This work was supported by the National Natural Science Foundation of China (Grant Nos. 51472038 and 11904041), the Nature Science Foundation of Chongqing (Grant Nos. cstc2019jcyj-msxmX0566, cstc2019jcyjmsxmX0237, cstc2018jcyjA2923, cstc2017jcyjAX0393, cstc2018jcyjAX0450, cstc2015jcyjA50035 and cstc2015jcyjA1660), the Scientific and Technological Research Program of Chongqing Municipal Education Commission (Grant Nos. KJ1703042, KJ1500319, KJ1501112, KJKJQN201800102, KJQN201800619), the Fundamental Research Funds for the Central Universities (2019CDXYWL0029,2018CDJDWL0011, 106112017CDJQJ328839, 106112016CDJZR288805 and 106112015CDJXY300002), the opening project of State Key Laboratory of Luminescence and Applications (SKLA-2019-) and Chongqing Key Laboratory of Micro /Nano Materials Engineering and Technology (KFJJ1301), Opening Foundation of Chongqing Key Laboratory of Photoelectric Functional Materials (CS201807), and the Sharing Fund of Large-scale Equipment of Chongqing University (Grant No. 201903150094), and the Foundation for the Creative Research Groups of Higher Education of Chongqing (No. CXTDX201601016). We also thank Analytical and Testing Center of Chongqing University for performing XRD, XPS and SEM tests.

References

[1] U. Özgür, Y.I. Alivov, C. Liu, A. Teke, M.A. Reshchikov, S. Doğan, V. Avrutin, S.J. Cho, H. Morkoç, A comprehensive review of ZnO materials and devices, J. Appl. Phys. 98 (2005) 041301. https://doi.org/10.1063/1.1992666

[2] S.B. Zhang, S.H. Wei, A. Zunger, Intrinsic n-type versus p-type doping asymmetry and the defect physics of ZnO, Phys. Rev. B 63 (2001) 075205. https://doi.org/10.1103/PhysRevB.63.075205

[3] V. Avrutin, D.J. Silversmith, H. Morkoç, Doping asymmetry problem in ZnO: current status and outlook, Proc. IEEE 98 (2010) 1269-1280. https://doi.org/10.1109/JPROC.2010.2043330

[4] C.H. Park, S.B. Zhang, S.-H. Wei, Origin of p-type doping difficulty in ZnO: The impurity perspective, Phys. Rev. B 66 (2002) 073202. https://doi.org/10.1103/PhysRevB.66.073202

[5] A. Tsukazaki, A. Ohtomo, T. Onuma, M. Ohtani, T. Makino, M. Sumiya, K. Ohtani, S.F. Chichibu, S. Fuke, Y. Segawa, H. Ohno, H. Koinuma, M. Kawasaki, Repeated temperature modulation epitaxy for p-type doping and light-emitting diode based on ZnO, Nat. Mater. 4 (2005) 42-46. https://doi.org/10.1038/nmat1284

[6] E. Guziewicz, E. Przezdziecka, D. Snigurenko, D. Jarosz, B.S. Witkowski, P. Dluzewski, W. Paszkowicz, Abundant acceptor emission from nitrogen-doped Zno films prepared by atomic layer deposition under oxygen-rich conditions, ACS Appl. Mater. Interfaces 9 (2017) 26143-26150. https://doi.org/10.1021/acsami.7b04127

[7] J.L. Lyons, A. Janotti, C.G. Van de Walle. Why nitrogen cannot lead to p-type conductivity in ZnO. Appl. Phys. Lett. 95 (2009) 252105. https://doi.org/10.1063/1.3274043

[8] L. Liu, J.L. Xu, D.D. Wang, M.M. Jiang, S.P. Wang, B.H. Li, Z.Z. Zhang, D.X. Zhao, C.X. Shan, B. Yao, D.Z. Shen, p-Type conductivity in n-doped ZnO: the role of the N_{Zn}–V_O complex. Phys. Rev.

Lett.105 (2012) 215501. https://doi.org/10.1103/PhysRevLett.108.215501

[9] H. Shen, C.X. Shan, J.S. Liu, B.H. Li, Z.Z. Zhang, D.Z. Shen, Stable p-type Zn O films obtained by lithium-nitrogen codoping method. Phys. Status Solidi B250 (2013) 2102-2105. https://doi.org/10.1002/pssb.201300015

[10] R. Swapna, M.C. Santhosh Kumar, Deposition of Na-N dual acceptor doped p-type ZnO thin films and fabrication of p-ZnO:(Na, N)/n-ZnO:Eu homojunction. Mater. Sci. Eng., B 178 (2013) 1032-1039. https://doi.org/10.1016/j.mseb.2013.06.010

[11] C.Y. Kong, G.P. Qin, H.B. Ruan, M. Nan, R.J. Zhu, T.L. Dai, Effect of post-annealing on microstructural and electrical properties of N^+ ion-implanted into ZnO: In films. Chin. Phys. Lett. 25 (2008) 1128. https://doi.org/10.1088/0256-307X/25/3/087

[12] S.L. Yao, J.D. Hong, C.T. Lee, C.Y. Ho, D.S. Liu, Determination of activation behavior in annealed Al–N codoped ZnO Films. J. Appl. Phys. 109 (2011) 103504. https://doi.org/10.1063/1.3587164

[13] H. Wang, H.P. Ho, J.B. Xu, Photoelectron spectroscopic investigation of nitrogen chemical states in ZnO:(N, Ga) thin films. J. Appl. Phys. 103 (2008) 103704.https://doi.org/10.1063/1.2921986

[14] A. Chen, H. Zhu, Y. Wu, M. Chen, Y. Zhu, X. Gui, Z. Tang, Beryllium-assisted p-type doping for ZnO homojunction light-emitting devices, Adv. Funct. Mater. 26 (2016) 3696-3702. https://doi.org/10.1002/adfm.201600163

[15] M. Chen, R. Xiang, L. Su, Q. Zhang, J. Cao, Y. Zhu, X. Gui, T. Wu, Z. Tang, Stabilization of p-type dopant nitrogen in BeZnO ternary alloy epitaxial thin films, J. Phys. D: Appl. Phys. 45 (2012) 455101. https://doi.org/10.1088/0022-3727/45/45/455101

[16] K. Tang, S.L. Gu, K.P. Wu, S.M. Zhu, J.D. Ye, R. Zhang, Y.D. Zheng, Tellurium assisted

realization of p-type N-doped ZnO. Appl. Phys. Lett. 96 (2010) 242101. https://doi.org/10.1063/1.3453658

[17] K. Nakahara, S. Akasaka, H. Yuji, K. Tamura, T. Fujii, Y. Nishimoto, D. Takamizu, A. Sasaki, T. Tanabe, H. Takasu, H. Amaike, T. Onuma, S. F. Chichibu, A. Tsukazaki, A. Ohtomo, M. Kawasaki, Nitrogen doped $Mg_xZn_{1-x}O$/ZnO single heterostructure ultraviolet light-emitting diodes on ZnO substrates. Appl. Phys. Lett. 97 (2010) 013501.https://doi.org/10.1063/1.3459139

[18] Z. Ye, H. He, L. Jiang, Co-doping: an effective strategy for achieving stable p-type ZnO thin films, Nano Energy 52 (2018) 527-540. https://doi.org/10.1016/j.nanoen.2018.08.001

[19] T.M. Barnes, K. Olson, C.A. Wolden, On the formation and stability of p-type conductivity in nitrogen-doped zinc oxide, Appl. Phys. Lett. 86 (2005) 112112. https://doi.org/10.1063/1.1884747

[20] J.G. Lu, Y.Z. Zhang, Z.Z. Ye, L.P. Zhu, L. Wang, B.H. Zhao, Q.L. Liang, Low-resistivity, stable p-type ZnO thin films realized using a Li–N dual-acceptor doping method, Appl. Phys. Lett. 88 (2006) 222114. https://doi.org/10.1063/1.2209191

[21] H. He, Y. Zhu, M. Lei, Z. Ye, Acceptor evolution in Na-implanted a-plane bulk ZnO revealed by photoluminescence, J. Appl. Phys. 122 (2017) 095701. https://doi.org/10.1063/1.5000240

[22] P. Fons, H. Tampo, A.V. Kolobov, M. Ohkubo, S. Niki, J. Tominaga, R. Carboni, F. Boscherini, S. Friedrich, Direct observation of nitrogen location in molecular beam epitaxy grown nitrogen-doped ZnO, Phys. Rev. Lett. 96 (2006) 045504. https://doi.org/10.1103/PhysRevLett.96.045504

[23] X.H. Li, H.Y. Xu, X.T. Zhang, Y.C. Liu, J.W. Sun, Y.M. Lu, Local chemical states and thermal stabilities of nitrogen dopants in ZnO film studied by temperature-dependent x-ray photoelectron spectroscopy, Appl. Phys. Lett. 95 (2009) 191903. https://doi.org/10.1063/1.3259644

[24] M. Petravic, P.N.K. Deenapanray, V.A. Coleman, C. Jagadish, K.J. Kim, B. Kim, K. Koike, S.

Sasa, M. Inoue, M. Yano, Chemical states of nitrogen in ZnO studied by near-edge X-ray absorption fine structure and core-level photoemission spectroscopies, Surf. Sci. 600 (2006) 81-85. https://doi.org/10.1016/j.susc.2006.01.015

[25] H. Zhang, C. Kong, W. Li, G. Qin, M. Tan, H. Ruan, L. Fang, Fabrication and characterization of p-type In–N codoped ZnMgO films, J. Mater. Sci.: Mater. Electron. 28 (2017) 9316-9321. https://doi.org/10.1007/s10854-017-6669-0

[26] G. Kresse, J. Furthmüller, Efficient iterative schemes for ab initio total-energy calculations using a plane-wave basis set, Phys. Rev. B 54 (1996) 11169-11186. https://doi.org/10.1103/PhysRevB.54.11169

[27] J.P. Perdew, K. Burke, M. Ernzerhof, Generalized gradient approximation made simple, Phys. Rev. Lett. 77 (1996) 3865-3868. https://doi.org/10.1103/PhysRevLett.77.3865

[28] P.E. Blöchl, Projector augmented-wave method, Phys. Rev. B 50 (1994) 17953-17979. https://doi.org/10.1103/PhysRevB.50.17953

[29] G. Henkelman, B.P. Uberuaga, H. Jónsson, A climbing image nudged elastic band method for finding saddle points and minimum energy paths, J. Chem. Phys. 113 (2000) 9901-9904. https://doi.org/10.1063/1.1329672

[30] C.J. Barnett, V. Mourgelas, J.D. McGettrick, T.G.G. Maffeis, A.R. Barron, R.J. Cobley, The effects of vacuum annealing on the conduction characteristics of ZnO nanorods, Mater. Lett. 243 (2019) 144-147. https://doi.org/10.1016/j.matlet.2019.02.005

[31] G. Perillat-Merceroz, F. Donatini, R. Thierry, P.H. Jouneau, P. Ferret, G. Feuillet, Structural recovery of ion implanted ZnO nanowires, J. Appl. Phys. 111 (2012) 083524. https://doi.org/10.1063/1.4704697

[32]Y.F. Li, B. Yao, Y.M. Lu, Y.Q. Gai, C.X. Cong, Z.Z. Zhang, D.X. Zhao, J.Y. Zhang, B.H. Li, D.Z.

Shen, X.W. Fan, Z.K. Tang, Biaxial stress-dependent optical band gap, crystalline, and electronic structure in wurtzite ZnO: Experimental and ab initio study. J. Appl. Phys. 104 (2008) 083516. https://doi.org/10.1063/1.3000601

[33] X.Y. Zhang, J.Q. Qin, Y.Y. Xue, P.F. Yu, B. Zhang, L.M. Wang, R.P. Liu, Effect of aspect ratio and surface defects on the photocatalytic activity of ZnO nanorods. Sci. Rep. 4 (2014) 4596. https://doi.org/10.1038/srep04596

[34] S.A. Ansari, M.M. Khan, S. Kalathil, A. Nisar, J. Lee, M.H. Cho, Oxygen vacancy induced band gap narrowing of ZnO nanostructures by an electrochemically active biofilm. Nanoscale 5 (2013) 9238-9246.https://doi.org/10.1039/C3NR02678G

[35]E. Przezdziecka, W. Lisowski, A. Reszka, A. Kozanecki, Evidence of magnesium impact on arsenic acceptor state: Study of ZnMgO:As molecular beam epitaxy layers, Appl. Surf. Sci. 435 (2018) 676-679. https://doi.org/10.1016/j.apsusc.2017.11.173

[36] Z.G. Geng, X.D. Kong, W.W. Chen, H.Y. Su, Y. Liu, F. Cai, G.X. Wang, J. Zeng, Oxygen vacancies in ZnO nanosheets enhance CO_2 electrochemical reduction to CO. Angew. Chem. Int. Ed., 2018, 57(21): 6054-6059. https://doi.org/10.1002/anie.201711255

[37] H. Zhang, W.J. Li, G.P. Qin, H.B. Ruan, D. Wang, J. Wang, C.Y. Kong, F. Wu, L. Fang, Surface ferromagnetism in ZnO single crystal. Solid State Commun., 292 (2019) 36-39. https://doi.org/10.1016/j.ssc.2019.01.021

[38] D. Elizabeth Pugel, R.D. Vispute, S.S.Hullavarad, T.Venkatesan, B.Varughese, Compositional origin of surface roughness variations in air-annealed ZnO single crystals. Appl. Surf. Sci., 254 (2008) 2220-2223.https://doi.org/10.1016/j.apsusc.2007.07.206

[39] M. Baek, D. Kim, K. Yong, Simple but effective way to enhance photoelectrochemical solar-

water-splitting performance of ZnO nanorod arrays: charge-trapping $Zn(OH)_2$ annihilation and oxygen vacancy generation by vacuum annealing. ACS Appl. Mater. Interfaces 9 (2017) 2317-2325. https://doi.org/10.1021/acsami.6b12555

[40] S.Q. Wei, Y. Zhang, J.X. Zhao, S.H. Dai, J.S. Sun, Z.C. Shao, Effect of Electrochemical Preparation and Silver Modification of ZnO on Its Photocatalysis, Surface Technology, 47(8) (2018) 58-63 (in Chinese). https://doi.org/10.16490/j.cnki.issn.1001-3660.2018.08.009

[41] B.B. Su, D.F. Su, Q.F. Gui, Influence of molecular adsorption and surface defects on ultraviolet detection of ZnO Film, Surface Technology, 44(12) (2015) 137-142 (in Chinese). https://doi.org/10.16490/j.cnki.issn.1001-3660.2015.12.022

[42] C.L. Perkins, S.-H. Lee, X. Li, S.E. Asher, T.J. Coutts, Identification of nitrogen chemical states in N-doped ZnO via x-ray photoelectron spectroscopy, J. Appl. Phys., 97 (2005) 034907. https://doi.org/10.1063/1.1847728

[43] C.W. Zou, X.D. Yan, J. Han, R.Q. Chen, W. Gao, J. Metson, Study of a nitrogen-doped ZnO film with synchrotron radiation, Appl. Phys. Lett., 94 (2009) 171903. https://doi.org/10.1063/1.3125255

[44] M. Futsuhara, K. Yoshioka, O. Takai, Structural, electrical and optical properties of zinc nitride thin films prepared by reactive rf magnetron sputtering, Thin Solid Films, 322 (1998) 274-281. https://doi.org/10.1016/S0040-6090(97)00910-3

[45] W. Li, C. Kong, G. Qin, H. Ruan, L. Fang, p-Type conductivity and stability of Ag–N codoped ZnO thin films, J. Alloys Compd., 609 (2014) 173-177. https://doi.org/10.1016/j.jallcom.2014.04.051

[46] A. Janotti, C.G. Van de Walle, Native point defects in ZnO, Phys. Rev. B, 76 (2007)165202 . https://doi.org/10.1103/PhysRevB.76.165202

[47]W. Li, C. Kong, H. Ruan, G. Qin, L. Fang, X. Meng, H. Zhang, P. Zhang, Q. Xu, Investigation on

the formation mechanism of In–N codoped p-type ZnCdO thin films: experiment and theory, The J. Phys. Chem. C, 118 (2014) 22799-22806. https://doi.org/10.1021/jp507724y

[48] Y.F. Wang, D.Y. Song, L. Li, B.S. Li, A. Chen, Y. Sui, Improvement of thermal stability of p-type ZnO:(Al, N) fabricated by oxidizing Zn_3N_2: Al thin films. Phys. Status Solidi C, 2016, 13(7-9): 585-589. https://doi.org/10.1002/pssc.201510164

Figure Caption:

Figure 1. XRD patterns of as-implanted and post-annealed ZnO:In-N films.

Figure 2. (a-e) The O 1*s* XPS spectra of as-implanted and post-annealed ZnO:In-N samples; (f) the calculated ratio of integral areas (O_{II}/O_I) as a function of annealing temperature (T_A).

Figure 3. (a-e) The high-resolution N 1*s* XPS spectra of as-implanted and post-annealed ZnO:In-N films; **(f)** the integral area versus annealing temperature (T_A).

Figure 4. SIMS profile of nitrogen dopants in ZnO:In-N film annealed at different temperatures.

Figure 5. Interaction between two adjacent N_O acceptors through different paths: **(a)** the first out of (0001) plane and **(b)** the first in (0001) plane. **(c)** Interactions between N_O acceptor and split-N_i. The inset shows initial and final configurations. Gray spheres, red spheres and blue spheres represent Zn, O and N atoms, respectively.

Figure 6. (a) Different diffusion paths in the ZnO wurtzite structure; **(b)** calculated diffusion energy barrier for the isolated V_O; and **(c)** calculated diffusion energy barrier for the neutral charge state of N_O via V_O-assisted diffusion mechanism. The diffusion path "B→A" is the first out of (0001) plane and the diffusion path "B→C" is the first in (0001) plane. Gray spheres are Zn atoms and red spheres represent the oxygen sites.

Figure 7. Calculated diffusion energy barrier for the $(N_2)_O$ via V_O-assisted diffusion mechanism. Gray spheres, red spheres and blue spheres are Zn, O and N atoms, respectively.

Fig. 1.

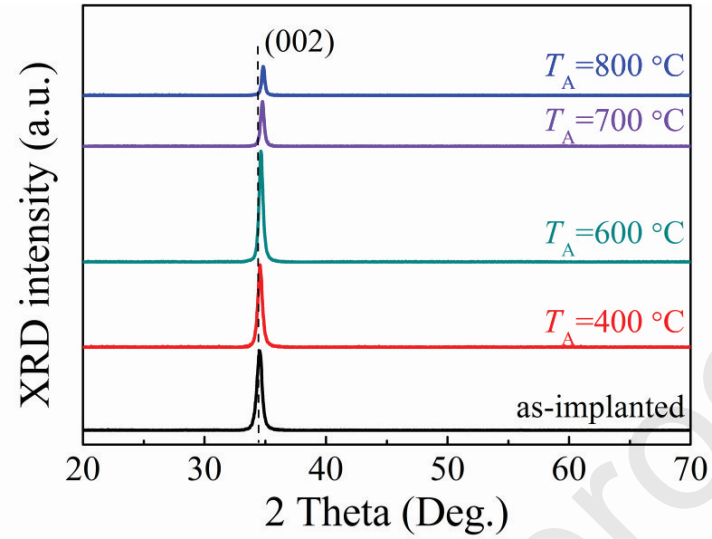

Fig. 2.

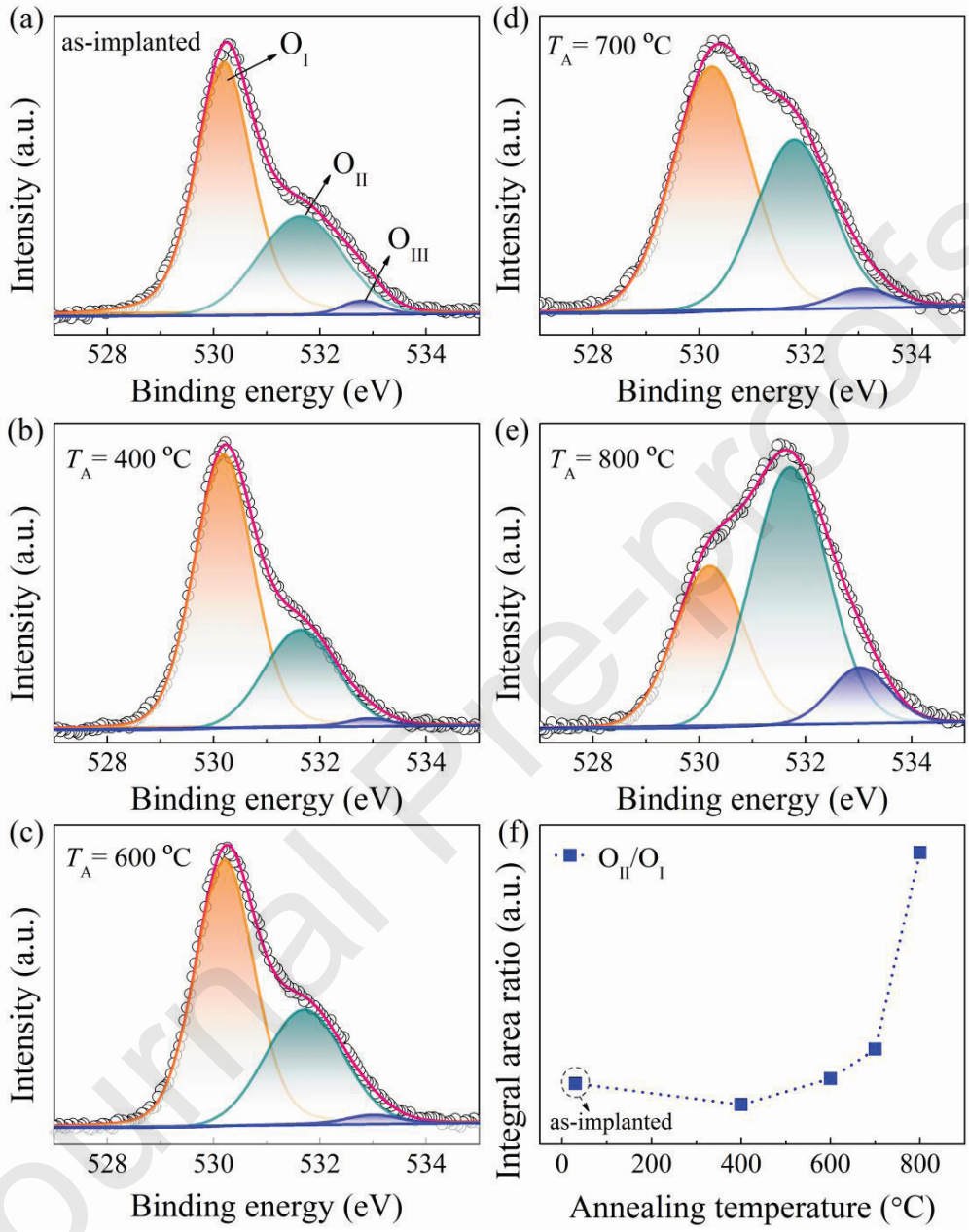

Fig. 3.

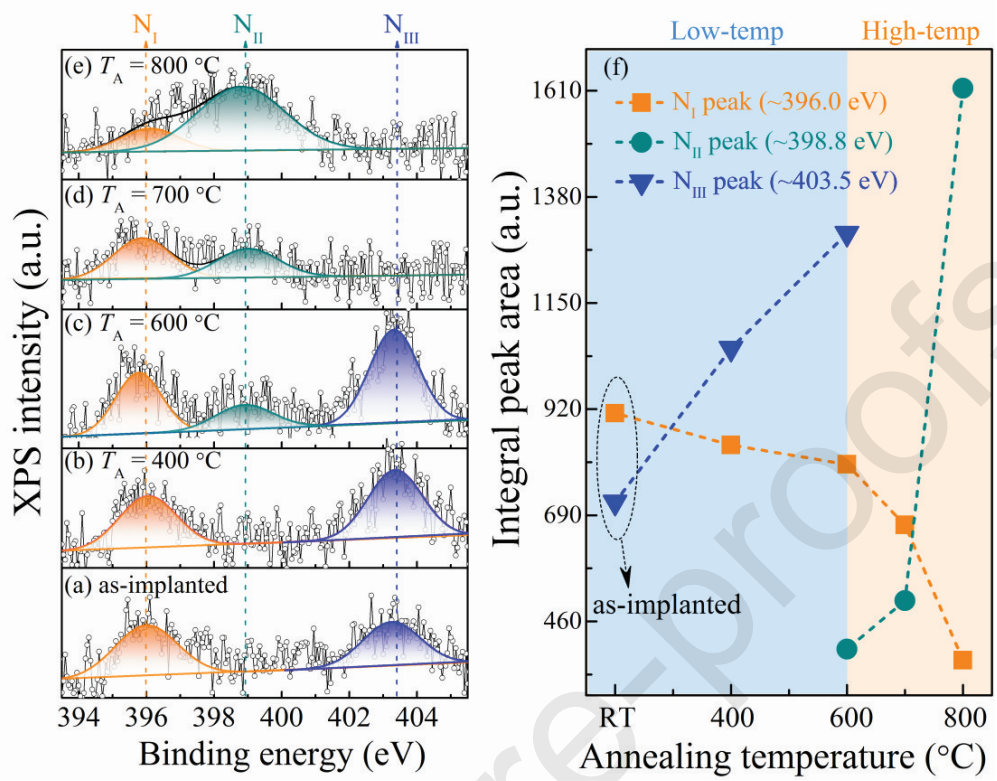

Fig. 4.

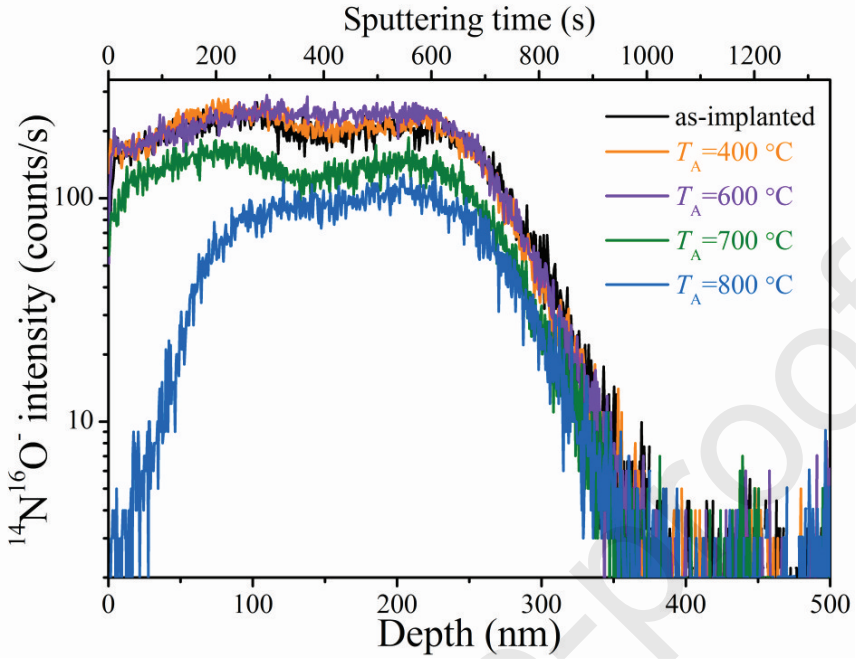

Fig. 5.

Fig. 6.

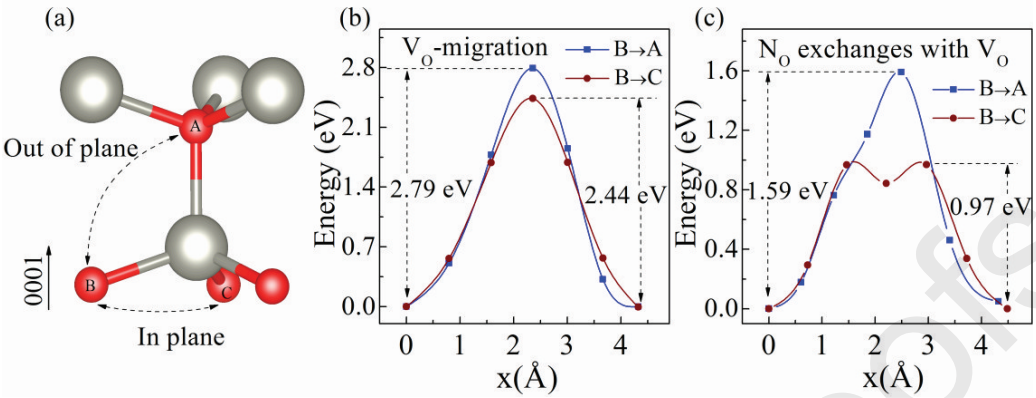

Fig. 7.

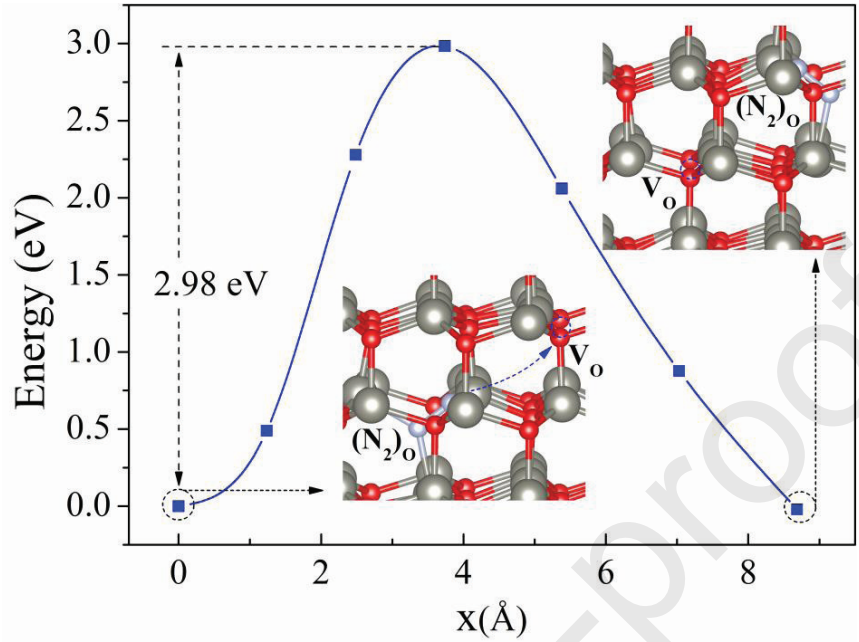

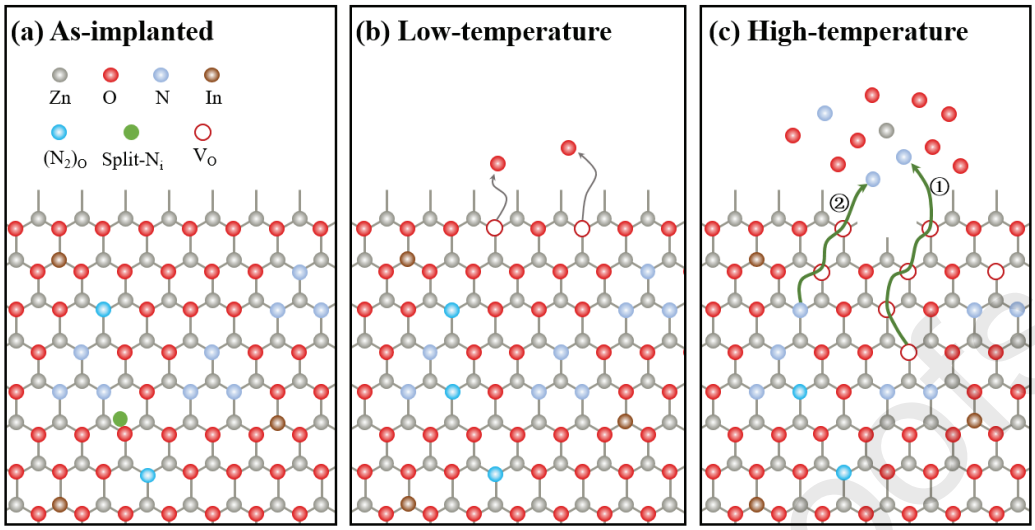

Schematic diagram of the thermal evolution and migration of N dopants in ZnO:In-N fims at different post-annealing temperature.

Highlights

1、 The evolution of N local environment strongly depends on the annealing temperature.

2、 Low-temperature annealing leads to the formation of additional $(N_2)_O$ donors.

3、 High-temperature annealing induces the generation of near surface oxygen vacancies.

4、 High-temperature annealing causes the serious out-diffusion of N dopants.

5、 The out-diffusion of N-dopants via vacancy-assisted mechanism is proposed.

Declaration of interests

☒ The authors declare that they have no known competing financial interests or personal relationships that could have appeared to influence the work reported in this paper.

☐The authors declare the following financial interests/personal relationships which may be considered as potential competing interests: